Available online at www.sciencedirect.com
ScienceDirect
Journal of Sound and Vibration 302 (2007) 892–902
JOURNAL OF SOUND AND VIBRATION
www.elsevier.com/locate/jsvi

Non-uniform heat generation in rods with hysteretic damping

D.D. Ebenezer[a,*], D. Thomas[a,b], S.M. Sivakumar[b]

[a]*Naval Physical and Oceanographic Laboratory, Thrikkakara, Kochi 682 021, India*
[b]*Department of Applied Mechanics, Indian Institute of Technology—Madras, Chennai 600 036, India*

Received 13 July 2006; received in revised form 9 December 2006; accepted 15 December 2006
Available online 23 February 2007

Abstract

Heat is generated and vibrational energy is dissipated when damped structures are excited. In certain applications, the associated increase in temperature is moderate but affects the performance of resonant vibrators and linear analysis is expected to provide insight. In this paper, lumped and distributed systems with losses are modelled and heat generation due to harmonic excitation is studied. The internal loss is modelled as hysteretic damping. First, a lumped mass-spring with loss represented by a complex spring constant is analysed. Analytical expressions for the frequency at which the maximum power is dissipated and the maximum power dissipated are derived. Next, a long, thin, viscoelastic rod with hysteretic damping represented by a complex Young's modulus is analysed. It is harmonically excited at one end and two different boundary conditions at the other end are considered. It is seen from the linear analysis that heat generation is spatially non-uniform and will affect the temperature distribution. Analytical expressions for the frequency at which the maximum power is dissipated and the maximum power dissipated are derived for a rod fixed at one end and excited at the other. It is also noted that frequency at which maximum power is dissipated increases as loss increases. The effect of loss factor on the dissipated power is also studied and numerical results are presented.

1. Introduction

Heat is generated and vibrational energy is dissipated when damped structures are excited. The resulting increase in temperature of the structure causes a change in its material properties. Therefore, there is a change in the response of the structure to the excitation.

It is often sufficient to determine the steady-state response—by iteration—when the excitation is harmonic. In the first step of the iteration, the heat generated is determined for an assumed temperature distribution and corresponding material properties. In the second step, the temperature distribution corresponding to the heat generated and thermal boundary conditions is determined. The iteration is stopped when the assumed temperature distribution in the first step is nearly equal to that computed in the second step. Linear analysis can be used in the first step when the material properties corresponding to the temperature distribution are nearly independent of spatial position even when there is a moderate increase in the average steady-state temperature. Some types of piezoelectric ceramics with electrical insulators—that are also good thermal

*Corresponding author. Fax: +91 484 2424858.
E-mail address: tsonpol@vsnl.com (D.D. Ebenezer).

0022-460X/$ - see front matter © 2007 Published by Elsevier Ltd.
doi:10.1016/j.jsv.2006.12.022

insulators—at the ends are examples of such structures. In this paper, linear analysis is used to determine the non-uniform heat generated in a rod.

Lumped, damped oscillators in steady state, linear motion are discussed in several books [1–3]. In viscous damping, the damping force is in phase with and proportional to the velocity. The heat generated per cycle is proportional to frequency and the square of the amplitude of the response but this is contrary to observations in viscoelastic materials [4]. When the damping force is in phase with velocity but proportional to displacement, the heat generated per cycle is independent of frequency but proportional to the square of the amplitude of the response. Muravskii [5], in a recent paper, states that the discovery of several engineering materials with frequency-independent damping was first reported in 1927 and provides several references to earlier work. This type of damping can be modelled using a complex spring constant. It is known as hysteretic damping, solid damping, or structural damping when the constant is assumed to be independent of frequency, temperature, etc. [2].

Distributed, damped structures can also be modelled using complex material properties. Several types of stress–strain relations such as stress proportional to strain as in elastic materials, strain rate as in viscous materials, a weighted sum of strain and strain rate as in viscoelastic materials, and other generalised ones can be modelled using complex material properties [6,7].

Steady state as well as transient analyses of distributed, damped structures have been reported in literature. Frequency-dependent material properties should be used in both cases to avoid violation of the Kramers–Kronig relations or causality condition. Material properties that are frequency-dependent are also temperature-dependent. However, it can be assumed that the damping is hysteretic if the properties are nearly independent of frequency in the neighbourhood of the frequency at which steady-state analysis is done and nearly independent of temperature in the neighbourhood of the average temperature of the rod. This approximation—used in this paper—makes it possible to analytically investigate heat generated in a viscoelastic rod using linear governing equations. However, when transient analysis is of interest, it is usually more convenient to use a stress–strain relation defined in the time domain.

Linear viscoelastic rod theory has been used in earlier studies. For example, Snowdon [8] studied rods excited at one end and with various boundary conditions at the other end. Pritz [9] studied rods with a mass at one end and specified displacement at the other end and, very recently, Gürgöze and Zeren [10] determined the eigencharacteristics of such rods. Buchanan [11] used linear equations to model viscoelastic rods and experimentally determine their complex Young's modulus. Tauchert [12] also used linear theory to analyse a rod undergoing torsional oscillations due to a specified shear-strain distribution. He computed the temperature distribution using Fourier series. Day [13] used linear equations to investigate thin plates. He showed that, in some cases with thermal excitation, the same final temperature distribution is obtained even if thermoelastic coupling is neglected in the energy equation.

The work presented in this paper is organised as follows. First, a lumped oscillator (mass-spring system) with hysteretic damping represented by complex stiffness is analysed. Expressions are derived for the frequency at which maximum power is dissipated (heat is generated) and the maximum power. Then, the rate at which heat is generated in a long, thin, viscoelastic rod is computed using two methods. The assumption that damping is hysteretic makes it possible to derive analytical expressions for the frequency at which maximum heat is generated and for the non-uniform distribution of heat generated along the length of the rod for different boundary conditions. Numerical results are presented to illustrate the spatial distribution of the heat generated and the effect of loss factor on the total rate at which heat is generated.

Heat generated due to vibration of damped structures is of interest because it is one of the reasons for the failure of piezoelectric ceramic transducers [14].

2. A lumped oscillator

Consider a lumped mass-spring system excited by a harmonic force, $f(t) = Fe^{j\omega t}$ as shown in Fig. 1. It is convenient to assume that F is real and independent of frequency. The displacement, $u(t) = U(\omega)e^{j\omega t}$, of the mass is

$$U(\omega)e^{j\omega t} = Fe^{j\omega t}/[K - \omega^2 M], \tag{1}$$

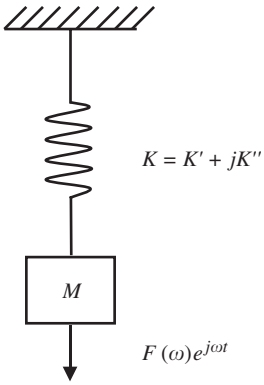

Fig. 1. A mass-spring system with hysteretic damping excited by a harmonic force.

where t denotes time, ω is the angular frequency of excitation, K is the constant stiffness of the spring, and M is the mass. Eq. (1) is valid for a lossless system but can be used to analyse a system with internal losses or damping by assuming that the stiffness is complex and is expressed as $K = K' + \mathrm{j}K''$ where K' and K'' denote the real and imaginary parts, respectively.

Only the real parts of the complex quantities used in Eq. (1) have physical significance. However, it is convenient to use the complex representation. For example, the velocity, $v(t)$, of the mass is expressed by using Eq. (1) as

$$V(\omega)\mathrm{e}^{\mathrm{j}\omega t} = \mathrm{j}\omega F\mathrm{e}^{\mathrm{j}\omega t}/[K - \omega^2 M]. \tag{2}$$

The incremental work done in driving the system is

$$\mathrm{d}w(t) = \mathrm{Re}(f(t))\,\mathrm{d}[\mathrm{Re}(u(t))], \tag{3}$$

and the power input to the system, averaged over one period, is

$$\Pi(\omega) = \frac{1}{T}\int_0^T \mathrm{d}w(t) = \frac{1}{T}\int_0^T \mathrm{Re}(f(t))\mathrm{Re}(v(t))\,\mathrm{d}t, \tag{4a}$$

where T is the period of the excitation. This power is dissipated in the form of heat. It is easily seen that

$$\Pi(\omega) = \frac{F^2 K''\omega}{2\left[(K' - \omega^2 M)^2 + K''^2\right]}. \tag{4b}$$

The average dissipated power can also be expressed as

$$\Pi(\omega) = |F|\left|V(\omega)\right|\cos(\theta)/2, \tag{5a}$$

where

$$\theta = \tan^{-1}[(K' - M\omega^2)/K''], \tag{5b}$$

is the phase angle between $\mathrm{Re}[f(t)]$ and $\mathrm{Re}[v(t)]$.

The average dissipated power can also be determined by an alternative graphical approach that is useful when it is experimentally determined. It is seen from Eqs. (3) and (4a) that $\Pi(\omega)$ is proportional to the area under the curve of $\mathrm{Re}[u(t)]$ vs. $\mathrm{Re}[f(t)]$. These curves, also known as hysteresis loops, are shown in Fig. 2 for the case where $M = 1$ and $K = (1 + j0.3)/(2\pi)^2$. Loops are shown at frequencies of 0.8, 1, and 1.2 Hz and correspond to below resonance, nearly resonance, and above resonance frequencies.

When analytical expressions are known for the force and displacement, the area under the loop can be analytically determined. Eq. (1) can then be rearranged to obtain

$$\alpha u' + (M\omega^2 - K')f' = K''\sqrt{F_0^2 - f'^2}, \tag{6}$$

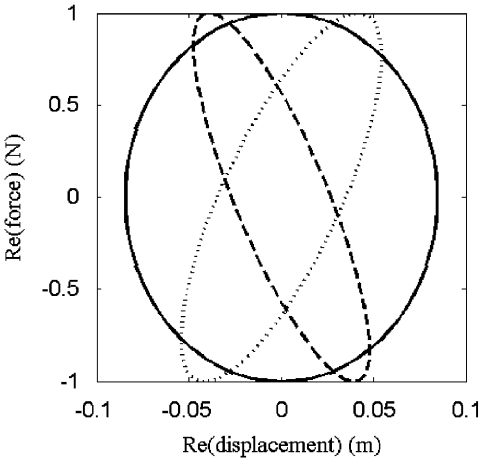

Fig. 2. Hysteresis loops of a mass-spring system with hysteretic damping excited with 1 N force at below resonance, nearly resonance, and above resonance at frequencies of 0.8 (dotted line), 1.0 (solid line), and 1.2 (dashed line) Hz, respectively.

where $\alpha = (K' - M\omega^2)^2 + K''^2$, $u' = \mathrm{Re}[u(t)]$ and $f' = \mathrm{Re}[f(t)] = F\cos\omega t$. Squaring both sides of Eq. (6) and rearranging yields

$$\alpha^2 u'^2 + 2\alpha(M\omega^2 - K')u'f' + \left[(M\omega^2 - K')^2 + K''^2\right]f'^2 - F^2K''^2 = 0. \tag{7}$$

Eq. (7) represents a rotated ellipse in the (u', f') plane. The major and minor axes coincide with the coordinate axes when it is rotated by an angle $\phi = 0.5\tan^{-1}[B/(A-C)]$ where A, B and C are the coefficients of u'^2, $u'f'$ and f'^2, respectively, in Eq. (7). It is noted that $\phi = 0$ at $\omega^2 = K'/M$, i.e., the major and minor axes coincide with the coordinate axes at the corresponding frequency. In Fig. 2, this occurs at 1 Hz. The major axis lies in the first and third quadrants at lower frequencies and in the second and fourth quadrants at higher frequencies. The area can be expressed in terms of the coefficients in Eq. (7).

The rate at which heat is generated by the system is A/T where A is the area of the ellipse. A is easily determined using standard formulae. It is shown later that both approaches yield the same numerical values for the average heat generation rate. When there is no loss K'' is zero, the major and minor axes are zero and power is also zero.

The angular frequency, ω_Π, at which Π is maximum is also the frequency at which $\mathrm{Re}(V(\omega) = |V(\omega)|\cos(\theta)$ is maximum, i.e., when

$$\frac{\mathrm{dRe}(V)}{\mathrm{d}\omega} = \frac{(K' - M\omega^2)^2 + K''^2 - 2(K' - M\omega^2)(-2M\omega)\omega}{(K' - M\omega^2)^2 + K''^2} = 0, \tag{8}$$

where it is assumed that the stiffness is independent of frequency in the neighbourhood of $\omega_\Pi/2\pi$. Assuming that the denominator is not zero and equating the numerator of the above equation to zero yields

$$\omega_\Pi^2 = \frac{K' \pm \sqrt{4K'^2 + 3K''^2}}{3M}, \tag{9}$$

where only the positive square root is considered because it yields a real frequency. When K'' is zero, the above equation is not valid because it reduces to $\omega_\Pi^2 = K'/M$ and the denominator of Eq. (9) is also zero at the same frequency and the assumption regarding the denominator is violated. In fact, as observed earlier, Π is zero at all frequencies when K'' is zero.

It is useful to relate ω_Π to other frequencies that can be easily measured. The angular frequency ω_V at which $|V(\omega)|$ is maximum is

$$\omega_V^2 = \frac{\sqrt{K'^2 + K''^2}}{M}. \tag{10}$$

Similarly, the angular frequencies ω_U and ω_A at which the magnitudes of displacement and acceleration are maximum, respectively, are found to be

$$\omega_U^2 = K'/M, \tag{11}$$

and

$$\omega_A^2 = \frac{K'^2 + K''^2}{K'M}. \tag{12}$$

It is seen from Eqs. (9)–(12) that

$$\omega_U < \omega_\Pi < \omega_V < \omega_A. \tag{13}$$

The maximum rate at which heat is generated by the system, $\Pi_{\max}$, is determined by substituting $\omega = \omega_\Pi$ in Eq. (4b). This yields

$$\Pi_{\max} \approx F^2(\omega)\left(K'/M\right)^{1/2}/2K'', \tag{14}$$

when $(4K'^2 + 3K''^2)^{0.5} \approx 2K'(1 + 3\eta^2/8)$ where $\eta = K''/K'$ and $K'' \ll K'$. It is of interest to note that $\Pi_{\max}$ increases when K'' decreases because the amplitude of vibration increases. Further, $\omega_\Pi^2 \approx K'/M$ when $\eta \ll 1$ and nearly corresponds to the frequency at which the axes of the ellipse coincide with the coordinate axes.

3. Rod with hysteretic damping

Consider a viscoelastic rod of cross-sectional area α and length L. The density of the rod is ρ and internal losses are represented by complex Young's modulus, $Y = Y' + \mathrm{j}Y''$. The rod is driven by a frequency-independent harmonic stress $\tau(L,t) = \tau(L,\omega)\mathrm{e}^{\mathrm{j}\omega t}$ at one end. Two different boundary conditions at the other end are considered. The non-uniform heat generated in the rod is of interest.

The average power input to the system is equal to the rate at which heat is generated and is determined using two approaches. In the first approach, it is determined by considering the force and displacement at the drive-point, as was done in the previous section. In the second approach, it is determined by integrating the local work done over the length of the rod.

The equation of motion for the rod is expressed in terms of the displacement, u, as

$$\frac{\partial^2 u(x,t)}{\partial t^2} = c^2 \frac{\partial^2 u(x,t)}{\partial x^2}, \tag{15a}$$

where

$$c^2 = Y/\rho. \tag{15b}$$

3.1. Rod fixed at $x = 0$ and driven at $x = L$

Consider the rod shown in Fig. 3. Solving Eqs. (15a) and (15b) and applying the boundary conditions yields

$$u(x,t) = \frac{\tau(L,\omega)\mathrm{e}^{\mathrm{j}\omega t}}{kY\cos(kl)}\sin(kx), \tag{16}$$

where $k = \omega/c$. Expressions for the velocity and strain are easily obtained when the Young's modulus is independent of frequency.

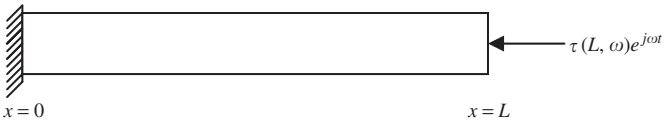

Fig. 3. Harmonically excited 1-D rod.

Consider the first approach. The time-averaged rate at which heat is generated in the rod is obtained by using Eq. (5a) and expressed as

$$\Pi(\omega) = \frac{\mathrm{A}}{T}\int_0^T \mathrm{Re}[\tau(t)]\mathrm{Re}[v(L,t)]\mathrm{d}t = \mathrm{T}^2(L,\omega)\mathrm{A}\left|\mathrm{j}(1/Y\rho)^{0.5}\tan(kL)\right|\cos(\vartheta)/2, \tag{17}$$

where $v(x,t)$ is the velocity and $\vartheta = \tan^{-1}[\mathrm{Im}(V(L,\omega))/\mathrm{Re}(V(L,\omega))]$.

The angular frequency, ω_Π, at which the dissipated power is maximum and the maximum dissipated power are of interest. The prescribed stress is independent of frequency and it is, therefore, seen from Eq. (17) that there is a local maximum in the power when $\mathrm{Re}(V(L,\omega))$ is maximum. After defining $\mathrm{j}/Y^{0.5} = g + \mathrm{j}h$ it is seen that ω_Π is obtained by solving

$$\frac{\mathrm{d}}{\mathrm{d}\omega}\Pi(\omega) = \frac{\tau^2(L,\omega)\alpha}{2\rho^{0.5}}\frac{\mathrm{d}}{\mathrm{d}\omega}\mathrm{Re}\left[(g+\mathrm{j}h)\frac{\sin(2k'L)+\mathrm{j}\sinh(2k''L)}{\cos(2k'L)+\cosh(2k''L)}\right] = 0. \tag{18}$$

In the lossless case, ω_V is the angular frequency at which $kL = \pi/2$. Therefore, it is assumed that $2k'L$ is a little less than π at ω_Π because of Eq. (12). Further, it is assumed $2k''L \ll 1$ because losses are small. Then, Eq. (18) reduces to

$$\frac{\mathrm{d}}{\mathrm{d}\omega}\Pi(\omega) \approx \frac{\tau^2(L,\omega)\alpha}{2\rho^{0.5}}\frac{\mathrm{d}}{\mathrm{d}\omega}\mathrm{Re}\left[\frac{g\pi}{(\pi-2k'L)^2+(2k''L)^2}\right] = 0, \tag{19}$$

and is solved to obtain

$$\omega_\Pi = \frac{\pi h}{2L\rho^{1/2}(g^2+h^2)}. \tag{20}$$

After defining $\eta = Y''/Y'$ and using

$$\mathrm{j}/Y^{0.5} = g + \mathrm{j}h \approx \frac{Y'^{0.5}Y''}{2\left(Y'^2+Y''^2\right)} + \mathrm{j}\frac{Y'^{1.5}}{Y'^2+Y''^2}(1+0.5\eta^2), \tag{21}$$

it is seen that

$$\omega_\Pi \approx \frac{\pi Y'^{0.5}}{2L\rho^{0.5}}(1+0.25\eta^2), \tag{22}$$

and

$$\Pi_{\max} \approx \frac{2\tau^2(L,\omega)\alpha}{\pi\rho^{0.5}}\frac{Y'^{0.5}}{Y''}(1+0.25\eta^2), \lhd \tag{23}$$

where, as in the lumped oscillator, $\Pi_{\max}$ is large when the loss Y'' is small.

In the second approach, the time-averaged rate at which heat is generated is expressed as

$$\Pi(\omega) = \frac{\alpha}{\tau}\int_0^L\int_0^T \mathrm{Re}[\tau(x,t)]\mathrm{Re}\left[\frac{\mathrm{d}s(x,t)}{\mathrm{d}t}\right]\mathrm{d}t\,\mathrm{d}x, \tag{24a}$$

where

$$\tau(x,t) = Ys(x,t) = \frac{\tau(L,\omega)\mathrm{e}^{\mathrm{j}\omega t}}{\cos(kL)}\cos(kx), \tag{24b}$$

is the stress. The integral over time in Eq. (24a) is easily performed to obtain

$$\Pi(\omega) = \alpha\int_0^L Q(x,\omega)\mathrm{d}x, \tag{25a}$$

where

$$Q(x,\omega)=\tau^2(L,\omega)\left|\mathrm{j}/Y\right|\omega\frac{\left|\cos(kx)\right|^2\cos(\varphi)}{2\left|\cos(kL)\right|^2}, \tag{25b}$$

is the time-averaged rate at which heat is generated per unit volume and $\varphi=\tan^{-1}(Y'/Y'')$ is the phase angle between stress and strain rate. It is seen by comparing Eqs. (15a), (15b), (24b), and (25b), that maximum heat is generated at the locations at which stress is maximum and displacement is minimum.

The integral over x in Eq. (25a) is analytically determined to obtain

$$\Pi(\omega)=\frac{A\tau^2(L,\omega)\omega\cos(\varphi)\left[k'\sinh(2k''L)+k''\sin(2k'L)\right]}{8k'k''\sqrt{Y'^2+Y''^2}\left[\cosh^2(k''L)-\sin^2(k'L)\right]}, \tag{26}$$

and, as expected, is in agreement with the result in Eq. (17).

The rate of heat generation, $Q(x,\omega)$, is of interest because it is required to determine the temperature distribution.

3.2. Rod free at $x=0$ and driven at $x=L$

The two coefficients in the solution to Eqs. (15a) and (15b) are determined by satisfying the zero stress boundary condition at $x=0$ and the specified force condition at $x=L$. The displacement in the rod is then expressed as

$$u(x,t)=-\tau(L,\omega)\mathrm{e}^{\mathrm{j}\omega t}\frac{\cos(kx)}{kY\sin(kl)}, \tag{27}$$

and expressions for strain, $s(x,t)$, and stress, $\tau(x,t)$, are obtained using it.

The time-averaged rate of total heat generated, obtained using the first approach, is

$$\Pi(\omega)=\frac{A}{T}\int_0^T\mathrm{Re}(\tau(L,t))\mathrm{Re}(v(L,t))\mathrm{d}t=\tau^2(L,\omega)A\left|\mathrm{j}(1/Y\rho)^{0.5}/\tan(kL)\right|\cos(\varphi)/2. \tag{28}$$

In the second approach, the average rate at which heat is generated is obtained by using Eq. (24a) where

$$Q(x,\omega)=\tau^2(L,\omega)\left|\mathrm{j}/Y\right|\omega\frac{\left|\sin(kx)\right|^2}{2\left|\sin(kL)\right|^2}\cos(\varphi). \tag{29}$$

The integral over the length of the rod is then analytically determined to obtain

$$\Pi(\omega)=\frac{\tau^2(L,\omega)A\omega\cos(\varphi)\left[k'\sinh(2k''L)-k''\sin(2k'L)\right]}{8k'k''\sqrt{Y'^2+Y''^2}\left[\cosh^2(k''L)-\cos^2(k'L)\right]}. \tag{30}$$

It is shown, in the next section, that Eqs. (28) and (30) yield the same results.

4. Numerical results and discussion

Some numerical results are shown to illustrate the effect of internal losses and the heat generated. The viscoelastic rod has a length, L, of 100 mm and diameter of 10 mm. Its material properties are $Y'=60$ MPa, $\eta=0.3$, and $\rho=1600\,\mathrm{kg/m^3}$ and the amplitude of harmonic excitation is 100 kPa unless stated otherwise.

First, consider a rod fixed at $x=0$ and excited at $x=L$. The average power input to the rod and converted to heat is computed using Eqs. (17) and (26) and shown in Fig. 4. Both equations yield the same values at all frequencies. The effect of the loss factor, η, on the average rate at which heat is generated in the neighbourhood of the resonance frequency, $\omega_\Pi/2\pi$, is shown in Fig. 5. It is seen that ω_Π increases when η increases. The approximate values of $\omega_\Pi/2\pi$ computed using Eq. (22) are 484.4, 485.3, 489.0 and 495.0 Hz for $\eta=0.05$, 0.1, 0.2 and 0.3 respectively. These values are in good agreement with the values of 484.3, 484.8, 486.6, and 489.6 Hz obtained from Eq. (26). It is also seen that the average power at ω_Π increases when η

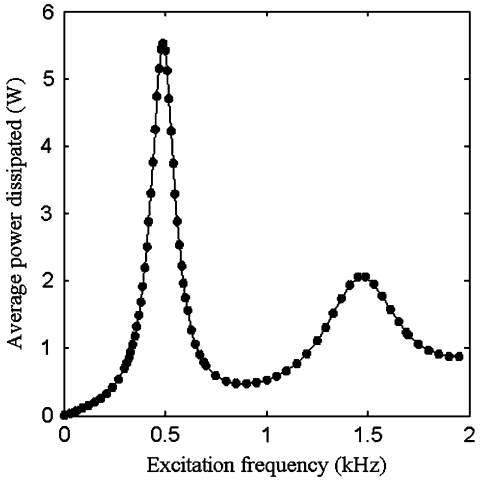

Fig. 4. Average power dissipated $\Pi(\omega)$ in a rod computed using two approaches. The rod is fixed at $x = 0$ and forced at $x = L$. Solid line: Eq. (17); dots: Eq. (26).

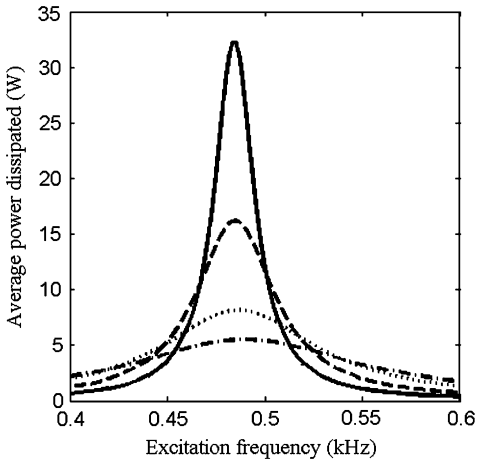

Fig. 5. Effect of loss factor, η, on the average power dissipated in a rod fixed at $x = 0$ and forced at $x = L$. Solid line: 0.05; dashed line: 0.1; dotted line: 0.2; dash-dot line: 0.3.

decreases. The approximate values of $\Pi_{\max}$ computed using Eq. (23) are 32.30, 16.18, 8.15 and 5.50 W for $\eta = 0.05$, 0.1, 0.2, and 0.3, respectively. These values are in good agreement with the values 32.30, 16.19, 8.17 and 5.53 obtained using Eq. (26) and Fig. 5. A similar figure for a spring-mass system with hysteretic damping is shown in Ref. [2].

The non-uniform heat generation rate is illustrated in Fig. 6 at various frequencies. The frequencies of 400, 490, 700, and 1470 Hz correspond to below first resonance, nearly first resonance, between first and second resonance, and nearly second resonance frequencies. It is seen that maximum heat is generated at the fixed end where stress is maximum for the first three frequencies. At the second resonance frequency, more heat is generated at an interior point than at the fixed end.

Next, consider a rod free at $x = 0$ and excited at $x = L$. The average rate at which heat is generated is computed using Eqs. (28) and (30) and shown in Fig. 7. Again, as expected, both approaches yield the same values at all frequencies. The non-uniform linear heat density is illustrated in Fig. 8 at various frequencies. The frequencies of 700, 980, 1500, and 1960 Hz correspond to below first resonance, nearly first resonance, between first and second resonance, and nearly second resonance frequencies. Here the heat generated is zero at $x = 0$

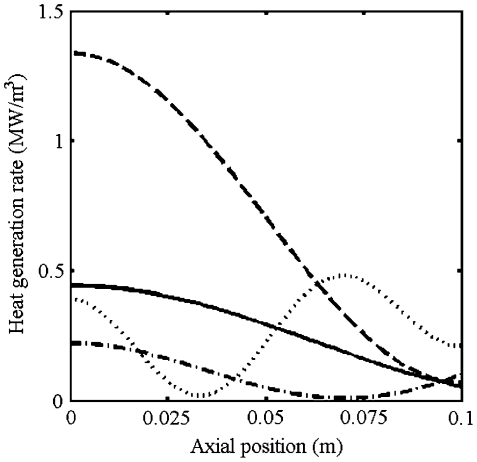

Fig. 6. Heat generation rate $Q(x,\omega)$ along the length of a rod driven at different frequencies. Rod fixed at $x=0$ and forced at $x=L$. Solid line: 400 Hz; dashed line: 490 Hz; dash-dot line: 700 Hz; dotted line: 1470 Hz.

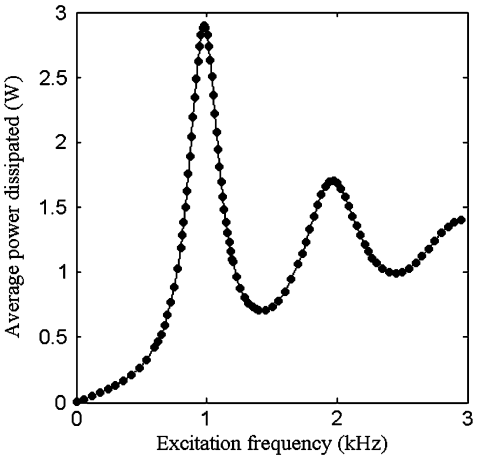

Fig. 7. Average power dissipated $\Pi(\omega)$ in a rod computed using two approaches. The rod is free at $x=0$ and forced at $x=L$. Solid line: Eq. (28); dots: Eq. (30).

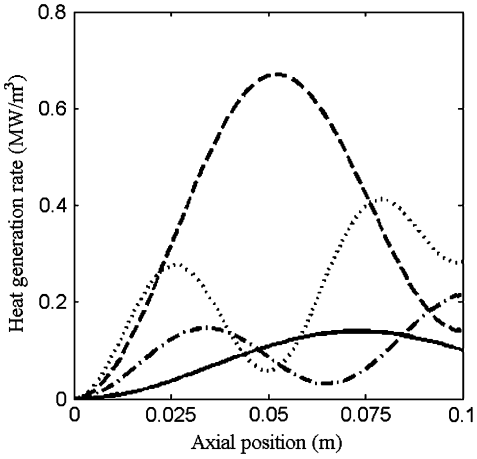

Fig. 8. Heat generation rate $Q(x,\omega)$ along the length of a rod driven at different frequencies. Rod free at $x=0$ and forced at $x=L$. Solid: 700 Hz; dashed: 980 Hz; dash-dot: 1500 Hz; dotted: 1960 Hz.

because it is stress free. At low frequencies, a local maximum occurs close to $x = L$ and shifts towards $x = 0$ as the frequency increases. Two local maxima occur as the frequency approaches the second resonance frequency and the second is greater than the first.

The numerical results are now used to draw general conclusions regarding the response of structures with low internal losses. Consider first a rod driven harmonically at an angular frequency ω_d that is equal to $\omega_{\Pi i}$. The latter is the angular frequency at which the rate of heat generation is maximum at the uniform initial temperature. When the rod is excited, the increase in temperature causes a change in the material properties and the angular frequency at which the rate of heat generation is maximum changes to $\omega_{\Pi f}$. This frequency is determined by iteration as explained earlier and is not equal to the drive frequency. Therefore, in the final or steady-state condition only a moderate amount of heat is generated in the low-loss rod because of the difference between ω_d and $\omega_{\Pi f}$ and the increase in temperature is also moderate.

Consider, next, a low-loss rod where Y' increases with temperature. It is driven harmonically at an angular frequency ω_d that is greater than $\omega_{\Pi i}$. When the rod is excited there is initially only a moderate increase in temperature because of the difference between ω_d and $\omega_{\Pi i}$. However, the angular frequency, ω_{Π}, at which the rate of heat generation is maximum will increase and approach ω_d. This will cause a further increase in temperature and thermal runaway can occur. It can also occur if Y' decreases with temperature and ω_d is less than $\omega_{\Pi i}$. This illustrates the importance of knowing the relationship between the drive frequency and ω_{Π} and the effect of temperature on Y.

5. Conclusions

The heat generated in lumped and distributed linear systems is investigated. A lumped mass-spring system with a complex spring constant and a one-dimensional (1-D) rod with complex Young's modulus are analysed. It is assumed that the complex constants are independent of frequency and temperature, i.e., hysteretic damping is present. Analytical expressions are derived for the heat generation rate and are used to determine maximum rate and the frequency at which it occurs. It is shown that the frequency increases when the damping increases.

In the lumped system, it is shown that the frequencies at which damped displacement, heat generation rate, damped velocity, and damped acceleration are maximum are in ascending order. This information is useful because displacement, velocity, and acceleration are easily determined experimentally and can be used to estimate or guide the search for the frequency at which maximum heat is generated. An expression for the maximum heat generated is also derived.

A viscoelastic rod with hysteretic damping represented by a complex Young's modulus is also analysed. The rod is excited at one end and two different boundary conditions are considered at the other end. In the first method, only the force and displacement at the driven end are used to determine the dissipated power. In the second, an expression for the heat generation rate is derived and integrated over the length of the rod to determine the total dissipated power. Heat generation rate is necessary to determine the temperature distribution in the rod and is, therefore, of interest. The temperature distribution depends on the thermal boundary conditions and can be analytically determined for certain cases.

Numerical results are presented to illustrate the total time-averaged power dissipated as a function of frequency, the increase in the frequency at which maximum heat is generated when the loss factor is increased, and the heat generation rate at various frequencies for two boundary conditions. The results are also used to show that knowledge of various resonance frequencies and the effect of temperature on Young's modulus can be used to avoid thermal runaway by choosing the drive frequency.

Work on extending the methods presented here to study heat generation in piezoelectric vibrators is in progress.

Acknowledgement

Encouragement and facilities given by Director, NPOL to carry out this work are gratefully acknowledged.

References

[1] J. Lazan, *Damping of Materials and Members in Structural Mechanics*, Pergamon, New York, 1968.
[2] D. Nashif, D.I.G. Jones, J.P. Henderson, *Vibration Damping*, John Wiley, New York, 1985.
[3] C.T. Sun, Y.P. Lu, *Vibration Damping of Structural Elements*, Prentice-Hall, New Jersey, 1995.
[4] D. Nashif, D.I.G. Jones, J.P. Henderson, *Vibration Damping*, John Wiley, New York, 1985, p. 42.
[5] G.B. Muravskii, On frequency independent damping, *Journal of Sound and Vibration* 274 (2) (2004) 653–668.
[6] J.C. Snowdon, Rubber like materials, their internal damping and role in vibration isolation, *Journal of Sound and Vibration* 2 (2) (1965) 175–193.
[7] L. Cremer, M. Heckl, E.E. Ungar, *Structure-borne Sound*, Springer Verlag, Berlin, 1972 (Chapter 3).
[8] J. Snowdon, Longitudinal vibration of internally damped rods, *Journal of the Acoustical Society of America* 36 (3) (1964) 502–510.
[9] T. Pritz, Dynamic strain of a longitudinally vibrating viscoelastic rod with an end mass, *Journal of Sound and Vibration* 85 (2) (1982) 151–167.
[10] M. Gürgöze, S. Zeren, On the eigencharacteristics of an axially vibrating viscoelastic rod carrying a tip mass and its representation by a single degree-of-freedom system, *Journal of Sound and Vibration* 294 (2006) 388–396.
[11] J.L. Buchanan, Numerical solution for the dynamic moduli of a viscoelastic bar, *Journal of the Acoustical Society of America* 81 (6) (1987) 1775–1786.
[12] T.R. Tauchert, Heat generation in a viscoelastic solid, *Acta Mechanica* 3 (1966) 385–396.
[13] W.A. Day, *Heat Conduction within Linear Thermoelasticity*, Springer Verlag, New York, 1985.
[14] D. Stansfield, *Underwater Electroacoustic Transducers*, Bath University Press, 1990.